ORIGINAL ARTICLE

Depth of dressing optimization in CBN wheels of different friabilities using acoustic emission (AE) technique

Felipe Aparecido Alexandre[1] · José Claudio Lopes[2] · Lucas de Martini Fernandes[2] ·
Fernando Sabino Fonteque Ribeiro[3] · Breno Ortega Fernandez[4] ·
Luiz Eduardo de Angelo Sanchez[2] · Rodolfo Fischer Moreira de Oliveira[5] ·
Hamilton José de Mello[2] · Paulo Roberto Aguiar[1] · Eduardo Carlos Bianchi[2]

Abstract

Grinding is a manufacturing process that has the objective of granting the workpiece a high-quality surface and is located at the end of the sequence of machining processes. During grinding operation, the abrasive grains of the wheel surface are worn and the pores are filled with debris. This phenomenon makes the cutting tool less efficient to remove material and sometimes improper to be used if a process to correct the cutting surface is not applied to the tool. Dressing is defined as a conditioning process which gives shape to the wheel and has the purpose of improving its capacity to remove material. In this context, this work proposes the monitoring of the dressing process of CBN wheels through acoustic emission technique (AE) along with the processing of digital signals. Dressing tests were done in a cylindrical grinder with two types of CBN wheels and the surface after the process was evaluated through micrographs. The AE signals were acquired with a 2 MHz sampling rate. In sequence, statistics such as RMS (root mean square) and counts were applied to the sample signals and analyses in the frequency domain were done to select frequency bands that are more related to the dressing process. The results show that the counts' analysis applied to the signals filtered in the selected bands is effective to detect the best moment to stop the dressing process.

Keywords Dressing process · Acoustic emission · CBN grinding wheel · Process monitoring

✉ Felipe Aparecido Alexandre
  felipe.alexandre@unesp.br

  José Claudio Lopes
  claudio.lopes@unesp.br

  Lucas de Martini Fernandes
  lucas-asewas@hotmail.com

  Fernando Sabino Fonteque Ribeiro
  fernando.ribeiro@ifpr.edu.br

  Breno Ortega Fernandez
  brenoortega@fpte.br

  Luiz Eduardo de Angelo Sanchez
  luiz.sanchez@unesp.br

  Rodolfo Fischer Moreira de Oliveira
  rodolfo.oliveira@saint-gobain.com

  Hamilton José de Mello
  hamilton.mello@unesp.br

  Paulo Roberto Aguiar
  paulo.aguiar@unesp.br

  Eduardo Carlos Bianchi
  eduardo.bianchi@unesp.br

[1] Department of Electrical Engineering, São Paulo State University "Júlio de Mesquita Filho", Bauru campus, Bauru, SP, Brazil

[2] Department of Mechanical Engineering, São Paulo State University "Júlio de Mesquita Filho", Bauru campus, Bauru, SP, Brazil

[3] Department of Control and Industrial Processes, Federal Institute of Education Science and Technology of Parana, Jacarezinho campus, Jacarezinho, PR, Brazil

[4] Department of Electrical Engineering, University of Lins, Lins campus, Lins, SP, Brazil

[5] Saint-Gobain Surface Conditioning, Department of Ceramic Materials, Guarulhos, SP, Brazil

1 Introduction

The manufacturing processes are essential to the economy. Currently, the increased need for manufacturing processes are more complex that require surface with higher quality, as well as the interconnection of industrial equipment is drastically increasing [1, 2]. The intelligent manufacturing will be able to rapidly adapt its structures to technology changes as manufacturing becomes faster, more precise, and more responsive to the customer needs [3, 4].

Grinding is a manufacturing process located at the end of the chain of the sequence of machining processes. This process is mostly used to grant the workpiece high-quality surface, well-defined geometric characteristics, and low roughness [5–11]. The cutting tool used in the grinding process is the grinding wheel, which has abrasive particles distributed randomly along its surface united by a bond material [12–14]. The structure of the tool makes the machining process harder to predict due to stochastic behavior [15] and it is known that the efficiency of the grinding process is highly dependent on the performance of the cutting tool [16–21]. During the grinding process, the abrasive grains on the cutting surface of the wheel undergo wear process and the pores are filled with chips that come from the material removed from the workpiece surface. This phenomenon makes the tool less efficient to remove material and sometimes improper to be used without a process to correct the cutting surface. In this context arises the need of the dressing process [22].

Dressing is defined as a conditioning process, which gives shape to the wheel and defines its capacity to remove material [23]. This process can be done in different ways including traditional techniques that use single-point or rotary dressers as well as with more recent methods such as electrolytic in-process dressing (ELID) and the laser dressing [24]. In the traditional dressing of conventional and CBN grinding wheels, the diamond dressers are commonly used as stationary tools. In this way, the sharpness of the grinding wheel surface obtained from dressing is strongly dependent on the parameters used in the process [25], which are mainly the dressing depth, feed rate, dresser type, and the number of passes [26, 27].

The grinding wheels are classified into two categories: conventional and superabrasive grinding wheels. The most used conventional wheels used are aluminum oxide and silicon carbide, while regarding superabrasives, cubic boron nitride (CBN) is commonly used. Regarding the cost, the superabrasive wheels will have from 10 to 100 times more expensive than aluminum oxide wheels [28], but have their cost compensated when analyzing the tool life and the heat dissipation efficiency during material removal from the workpiece surface during the grinding process.

The grinding wheel surface has an important role to define the ground workpieces roughness. If the grinding wheel is used improperly, damage on the workpiece surface may occur. In this context, the dressing process should be done accurately since it has a direct influence on the surface of the grinding wheel and therefore in the workpiece quality. Hence, the dressing process monitoring presents as a way to control the grinding wheel surface and the grinding process output parameters [29].

In many manufacturing industries that depend on the grinding process, the monitoring is done by a human operator [30, 31]. Most of the times, the operator stops the dressing process (the feed of the dresser in direction of the grinding wheel) to observe the grinding wheel surface condition. Hence, automatic monitoring systems are very important to the manufacturing industry, once it avoids human errors. In other words, it assists the process control and the accomplishment of a successful machining process [32].

Researchers have been putting efforts to establish diagnostic systems more precise using direct and indirect monitoring techniques [33]. The monitoring of the dressing process can be done using either of the techniques. The direct monitoring needs the interruption of the process since the measured variable is observed directly with high accuracy [34, 35]. On the other hand, indirect methods estimate the value of the desired variable through determined empiric correlations. In this way, it is less precise when comparing to direct methods but less complex and more proper for practical applications [36]. The most used sensors in the monitoring of the dressing process are the acoustic emission sensor (AE), force (dynamometer), vibration (accelerometer), and sensors to monitor power.

The monitoring of the dressing process has the main purpose of increasing quality control, reducing costs, and increasing productivity. Moreover, the monitoring of this process provides the operator the means to schedule the replacement of the dresser or of the grinding wheel in the correct time, avoiding damages to the manufactured components [5, 32]. Hence, this work has the objective of monitoring the dressing operation of CBN grinding wheels through acoustic emission technique and the digital processing of the signals.

Frequency domain studies were developed as well as frequency bands that better characterized the dressing process were selected. Besides that, the counts and the RMS statistics were applied to the original acoustic emission signals collected during the dressing process and also to the acoustic emission signals filtered in the selected frequency bands. The results indicate that the counts' statistic is effective in the identification of the moment that the dressing operation should be stopped, avoiding unnecessary material removal of the grinding wheel. It should be noticed that the dressing of CBN grinding wheels must be done carefully since it impacts considerably the performance of the process and the cost

of the tool is very high. Essentially, this is the reason for the development of this work.

There are works in the literature on monitoring the dressing process through acoustic signals and digital signal processing. However, no studies were found on the set composed by acoustic emission sensor digital signal processing applying frequency band analysis and statistics (RMS and Counts) in the monitoring of CBN wheels with different friability. This particularity makes this work interesting for the scientific and industrial community since the dressing of CBN wheels is often done incorrectly. These phenomena result in material waste or poor surface quality of parts. In this context, this work seeks to fill this gap with a simple monitoring proposal that uses standard statistics to monitor manufacturing processes.

The main contribution of this research that aggregate value to the research presented in [32] consists of the application of the RMS statistics, as well as presents a different type of grinding wheel that is monitored. While in [32] only one aluminum oxide grinding wheel is analyzed, in this work two CBN wheels with different friability characteristics are analyzed. In comparison to the work presented in [5], which monitors the shape of an aluminum oxide wheel using fuzzy systems, this work has a different approach since it monitors the dressing operation of CBN grinding wheels using statistics of low computational cost, resulting in a simpler monitoring system. In this way, this work presents an unprecedented approach regarding the monitoring of dressing of the CBN grinding wheels through acoustic emission and digital signal processing.

2 Monitoring of the dressing process

The measurement of the acoustic emission signal is considerably more sensitive to variations in the conditions of the grinding operation than measurements of force and power, resulting in a more promising technique for real-time measurement of the process [37]. According to [37], the acoustic emission signal sources during the process come mainly from the fracture of the bond/abrasive grain fracture and from the friction between the abrasive grain and the material which is in contact with it, mechanisms which are directly connected to the wear of the wheel.

Some notable advantages of the utilization of the acoustic emission sensor for monitoring are the tendency of the signal to propagate in frequencies much higher than the generated in the machining processes, minimizing the noises that are captured with the signal [8]. Given that, to analyze the friability aspect of the abrasive grains, the acoustic emission signal is the more proper parameter since it can capture precisely different signal magnitudes in function of different fracture modes, allowing reliable analysis.

The complexity of the grinding process requires continuous researches and various monitoring techniques are available to identify the problems that occur with this operation [38]. The monitoring of grinding processes through acoustic emission sensors is widely used nowadays [39]. In this context, some statistics are applied to the AE signal samples collected during the process. The main statistic used to evaluate the acoustic emission signals on the grinding process is the RMS [40–42], which is defined in Eq. 1:

$$AE_{rms} = \sqrt{\frac{1}{N}\sum_{i=1}^{N}AE^2(i)} \qquad (1)$$

where N is the block data size, AE is the raw acoustic emission signal, and i is the vector index of the raw AE signal.

Besides the RMS, other statistics can be used to analyze the acoustic emission signal, such as the rate of power (ROP) [43–45], the root mean square deviation (RMSD) [46], mean value deviation (MVD) [47], and the counts. According to [48], the counts' statistics is the number of times that the signal cross a threshold per unit time. This parameter can be used to quantify the acoustic activity of the signal.

The CBN grinding wheels are normally dressed with depth much lower than the aluminum oxide wheels since the dressing forces are much higher when using CBN [49]. In this way, monitoring of the dressing process is very important, especially when CBN grinding wheel is used [50]. With this, the loss of grinding wheel material can be minimized [51].

In this context, a monitoring system with combined sensors (Acoustic Emission and Power Sensors) was used to monitor the grinding process with CBN grinding wheels [51, 52]. The results showed that the use of this system along with digital signal processing techniques is effective in estimating the parameters of the cycles of the process, allowing optimization of the results. The power sensor was used aiming to evaluate the energy efficiency of grinding process with CBN wheels [53]. Besides the signals acquisition, roughness measures were taken to evaluate the performance of the tested tools. The results showed that this methodology is effective to evaluate the grinding wheels' performance and to assist in the selection of the wheel that is more proper to that specific process. The monitoring of the grinding process with CBN grinding wheels through SVM models and acoustic emission signals is presented by [54]. The results showed that the proposed system is capable of classifying the condition of the CBN wheel with an accuracy of 85%. Besides that, the authors showed that from the AE signal energy, it is possible to monitor the workpieces' roughness.

The monitoring of the dressing process is of great interest to the industry due to the added value the workpiece has at this point. The interruption of the grinding process, as well as the excessive loss of material, are factors that affect productivity. In this context, this work proposes a technique to monitor the
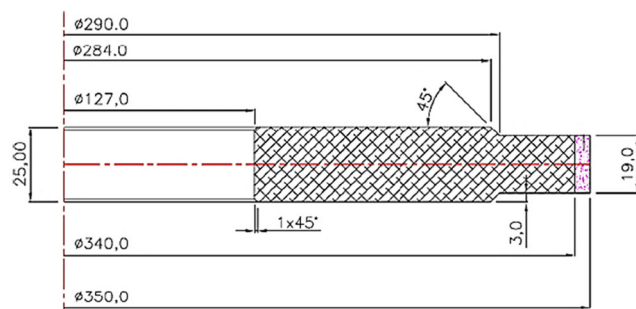
Fig. 1 Geometry and dimensions of the grinding wheel [55]

dressing of CBN wheels, optimizing the process regarding the waste of abrasive material and wheel performance. In this way, the implementation of this system can benefit both the manufacturing industry and the scientific community.

3 Material and methods

3.1 Experimental setup

The studies were developed in a cylindrical CNC grinder of SULMECÂNICA, model RUAP 515H, using a multi-point diamond dresser of Master Diamond ($15 \times 8 \times 10$) and two CBN grinding wheels with similar specifications, but an accentuated difference in the friability level of the abrasive grains, were used. The wheels are specified as SNB151.GS Q12 VR2 and SNB151.GL Q12 VR2 (known respectively as CBN GS and CBN GL).

The grinding wheels were manufactured with the following dimensions: 350 mm (outside diameter) $\times$ 19 mm (thickness) $\times$ 127 mm (hole diameter). The geometry and dimensions are presented in Fig. 1.

The acoustic emission sensor was positioned as indicated in Fig. 2 and the acquisition module Sensis DM42 was connected to the acquisition board of National Instruments, model BNC 2110. Although there is a
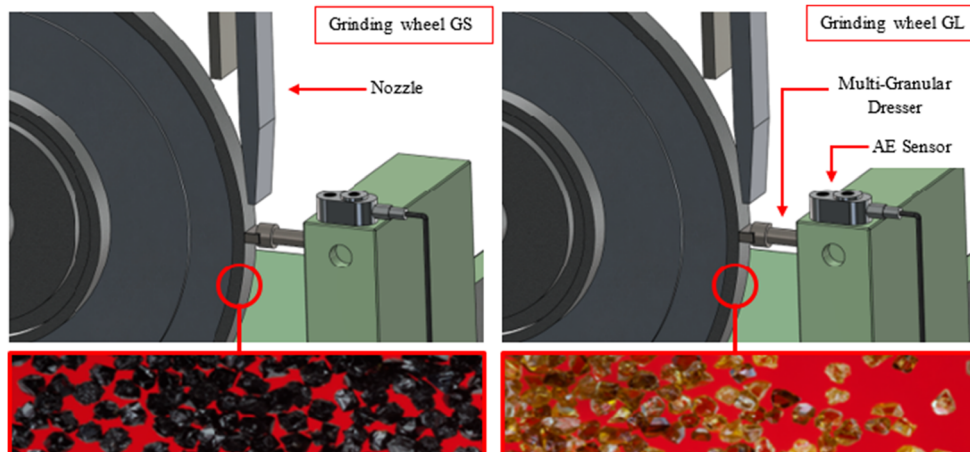
nozzle in the setup experiment (Fig. 2), the process occurred without using cutting fluid for the proper acquisition of the acoustic emission signals. As shown in Fig. 2, the sensor was positioned allowing the correct acquisition of the signals generated by the fracture of the abrasive grain/bond during the contact of the grinding wheel with the dresser. The tests consisted of dressing the CBN wheels moving the dresser longitudinally at a speed of 500 mm/min and using always depth of 1 μm, which is given by the approximation of the wheel towards the dresser after each pass.

Other data, as well as the main test parameters, are shown in Table 1.

3.2 Evaluation of the grinding wheel surface

After the execution of some passes of the grinding wheel over the dresser, micrographs of the wheel surface were taken to enable the further association of the intensity of the acoustic emission signal generated in a certain pass with the visual aspect of the wheel surface. Also, it was analyzed that the intensity of the clogging by the qualitative and quantitative identification of elements, such as the visibility of the abrasive grains, pores, and bonding materials or debris adhered to the surface.

The grinding wheel topography was analyzed before and after each test with an optical microscope, model DigiMicro Scale, produced by Dnt company, with $\times 200$ magnification, to verify the possible occurrence of the wheel clogging phenomenon.

3.3 Signal processing and selection frequency bands

Selecting frequency bands is a potent tool for monitoring manufacturing processes. By selecting frequency bands, it is possible to extract important characteristics of the monitored process, thereby achieve a diagnosis, whether about the tool or even the part being manufactured. According to Ribeiro et al.

Fig. 2 Schematic of the experimental setup showing the two different abrasive grains

Table 1 Parameters of the dressing test

Parameter	Description/value
Grinding wheel	Cubic boron nitride
Dresser	Multi-point diamond (15 mm × 8 mm × 10 mm)
Depth of cut	1 μm/pass
Longitudinal speed	500 mm/min
Cutting speed (v_s):	32 m/s
Grinding width:	4.5 mm
Cooling method	Dry

[46], the selection of frequency bands should be made by objective criteria, such as the low overlap of spectra between the conditions observed in the process, as well as evident differences in their amplitudes. These criteria guided the search for frequency bands in this work.

The acoustic emission signals (AE) obtained during the dressing process were processed digitally in MATLAB. Initially, the signals corresponding to the dressing passes were analyzed in the time domain with no application of digital processing. In sequence, it was applied that the RMS in all the dressing passes in blocks of 2048 points corresponds to 1 ms, as indicated in [37]. A low-pass digital filter of the type Butterworth with a cutoff frequency of 10 Hz and first-order was applied to the signals obtained from the RMS application aiming to eliminate the noisy frequencies, as indicated in [5]. Lastly, the RMS signal corresponding to the dressing pass was extracted and its average level was calculated for each dressing pass. In the same way of application of the RMS, the counts statistics was applied to the dressing signals in blocks of 2048 points, corresponding to 1 ms based on the research of [32]. A digital filter of low-pass Butterworth type with cutoff frequency of 10 Hz and order of filter 1 was applied to the signal with counts application. The average for each signal from the dressing passes was calculated.
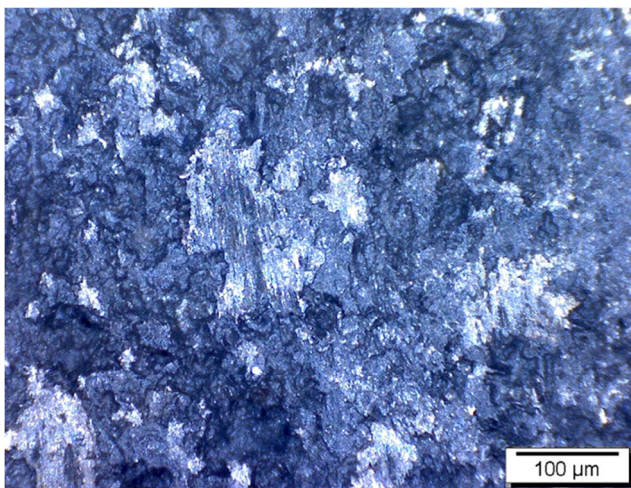

Fig. 3 GL grinding wheel in clogged condition
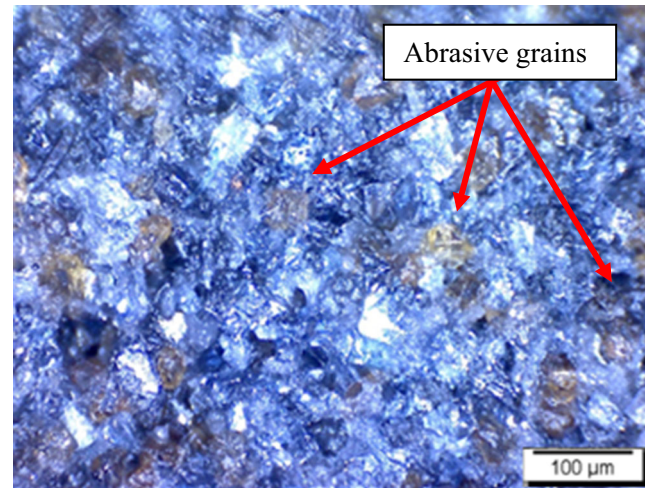

Fig. 4 GL grinding wheel dressed surface

After the analysis of the signal with the counts and RMS application, it was analyzed that the spectrum in signal frequency corresponds to the dressing passes. The objective of the signal processing is to find the frequency bands that are better related or characterize the behavior of the monitored process. The spectrum was obtained for three dressing conditions. The first pass represents the beginning of the dressing process in which the grinding wheel is clogged. The second pass corresponds to a sample obtained throughout the test, when it was removed part of the clogging of the wheel. Lastly, the third sample corresponds to the end of the dressing process, when the grinding wheel is not clogged anymore and is ready to be used in the process again. The fast Fourier transform (FFT) was obtained for the selected pass, using the fft command in the Matlab software and the Hanning window. Regarding the passes, the magnitude vectors of the spectrum in frequency were filtered using a digital filter Butterworth low pass filter with cutoff frequency of 2 kHz and order 4. This filter is necessary to allow a better analysis of the signal and to facilitate the searching of frequency bands, once it eliminates high frequency variations of magnitude of
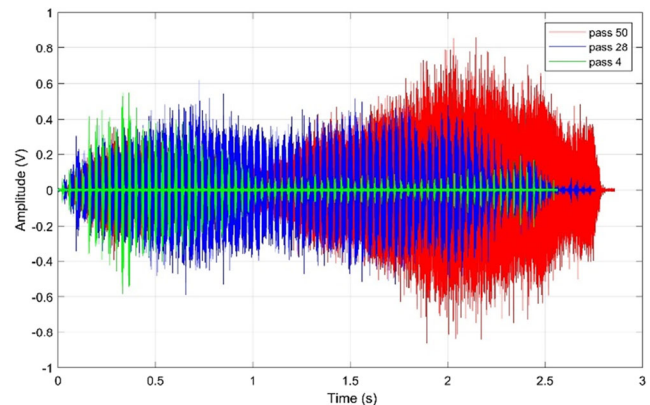

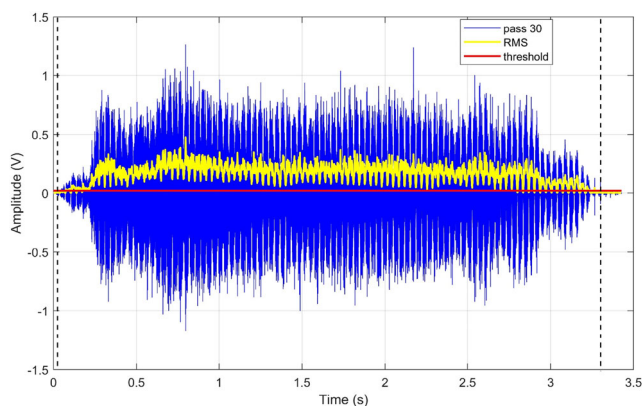**Fig. 5** Dressing passes signal on each condition (begging, during and end of the process)

Fig. 6 Parameters used to evaluate the tests

Fig. 8 Original signal *Counts*

the analyzed spectrum. A frequency band was selected using the criteria of non-superposition similar to the criteria presented in [12, 56, 57]. Afterwards, the AE signal of the dressing passes were filtered in the selected band through a digital band-pass filter Butterworth type and order 5. Lastly, the RMS and counts were applied again to the filtered signal in the selected band and the averages were obtained as described previously. The objective of applying it once again to the same statistics in the EA signal is to compare the obtained results looking for improvements in the diagnosis of the monitored process. It is important to highlight that the signal processing described in this section was applied to the signal of both CBN grinding wheels used in the tests and presented in the section "Experimental setup."

4 Results and discussion

4.1 Results for the grinding wheel GL—SNB151.GL Q12 VR2 (less friable abrasive grains)

4.1.1 Evaluation of the grinding wheel surface

The illustration of the GL grinding wheel in the clogged condition is presented in Fig. 3. Due to the fill of the wheel pores
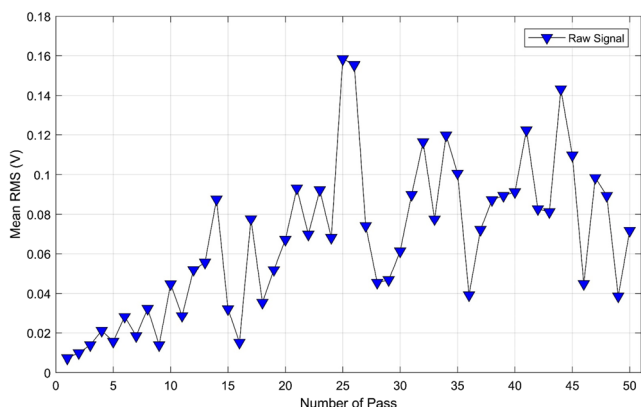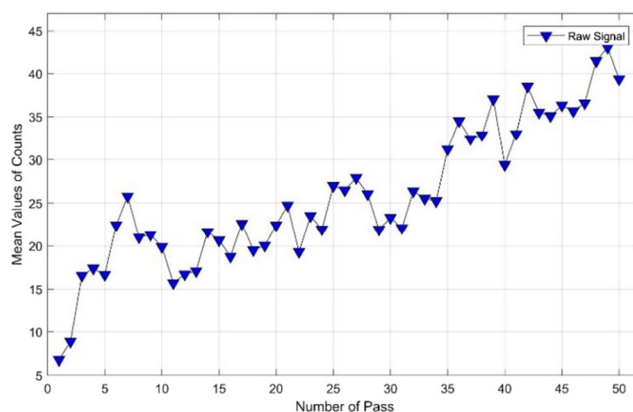

Fig. 7 Original RMS signal

with chips arose from the grinding process, it is not possible to see the abrasive grains on the wheel surface. This clogging condition makes the tool unfit to be used for the grinding operation once the abrasive grains' cutting edges are not able to efficiently remove material from the workpiece surface. Consequently, the grinding forces are increased and the process performance is impaired, resulting in workpieces with lower surface quality.

The dressing process restores the grinding wheel surface to the ideal condition removing a slight layer of the surface allowing the exposition of new cutting edges and the cleaning of the pores filled with debris. In this context, the wheel surface after the dressing process, described in the "Experimental setup" section, is presented in Figs. 4. This image was obtained from the wheel surface after 50 dressing passes. It is noteworthy that this topography may have been reached in previous steps. However, the process was not interrupted as standard industry operating conditions were sought. Thus, in future sections, it will be possible to observe that in some cases, some passes were made without necessity, resulting in the waste of the abrasive layer of the wheel, as well as of the diamonds that make up the dresser. Contrary to the previously shown condition, it is possible to identify the abrasive grains responsible for the material removal of the workpiece surface on the grinding process. Besides that, the abrasive grains present varied shapes, generally with sharp cutting edges, which is one of the parameters that define the capacity of the grinding wheel to remove material. The exposure of the abrasive grains and the cleaned pores allow the workpiece surface finish required to be attained and the process occurs more efficiently.

The analysis through images is very useful to determine the grinding wheel surface condition. However, it also has disadvantages, such as the considerable time needed to obtain a diagnosis and the need to interrupt the dressing or grinding process. Hence, the indirect monitoring through sensors is necessary to automatize these processes and support on the diagnosis of the wheel surface.

Fig. 9 Frequency band selection

(a)

(b)

(c)
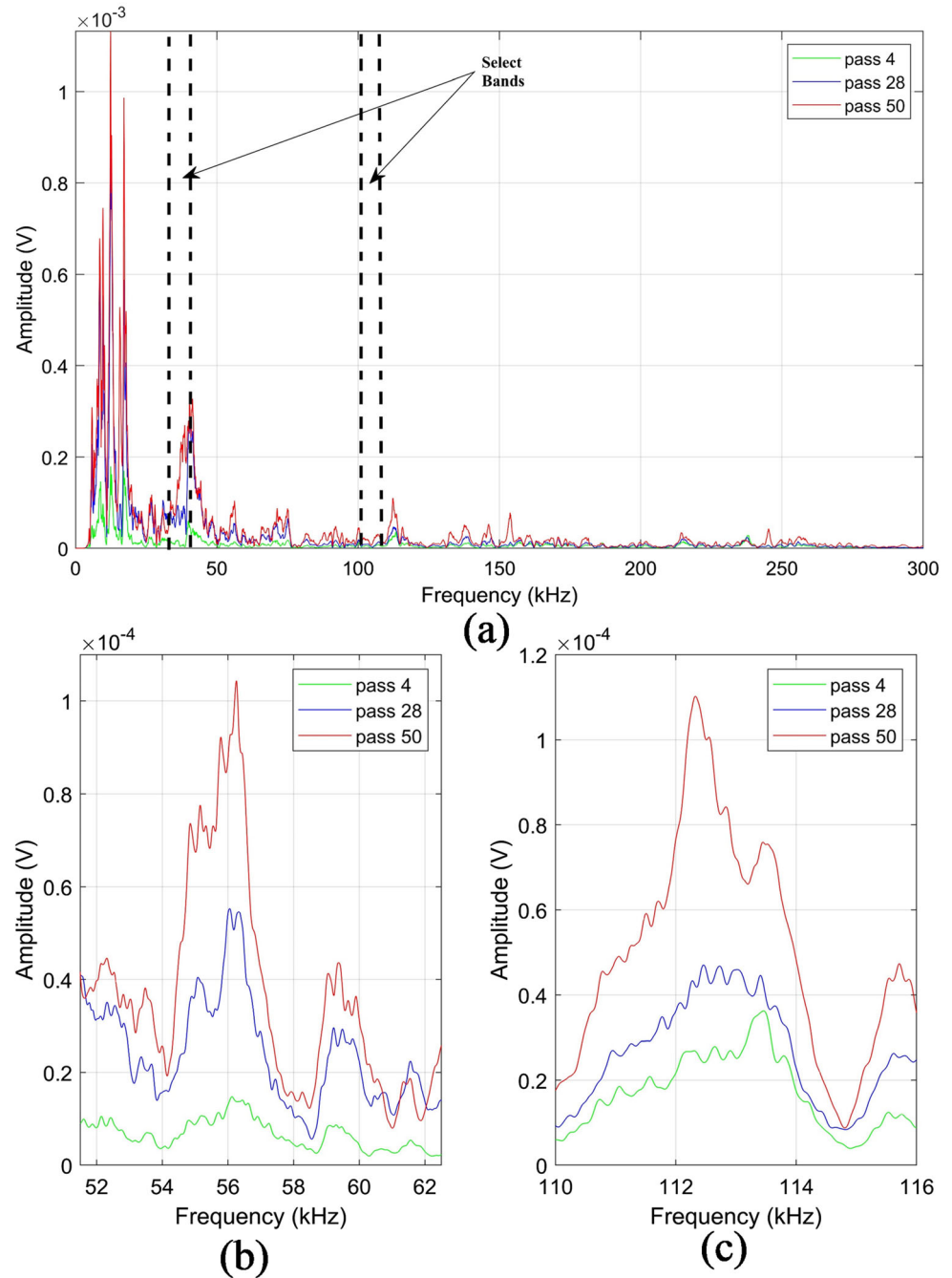
Regarding the dressing process, the operator stops it generally when there is no visual vestige of clogging and the tool is considered fit to be used again on the process. However, it is possible that the dressing process is stopped early and the tool still have not been conditioned properly to be used again or there is also a possibility of the operator interrupting the dressing process belatedly, obtaining the grinding wheel surface in the desired condition, but with a high associated cost due to unnecessary material removal of the tool surface, which proves the importance of an indirect monitoring of the process.

4.1.2 Digital processing of signal and band frequency selection

The acoustic emission signal obtained during the dressing process in three moments (beginning, random intermediate moment and final of the process) are shown in Fig. 5. It can be noted that the dressing signal of the fourth pass presents several spaced peaks originated from the irregular contact between the grinding wheel and the dressing tool. About the middle of the dressing process, which was analyzed as sample in the 28th pass, it can be observed the reduction of the

Fig. 10 Average RMS of the filtered signal. **a** 52–60 kHz band. **b** 110–116 kHz band
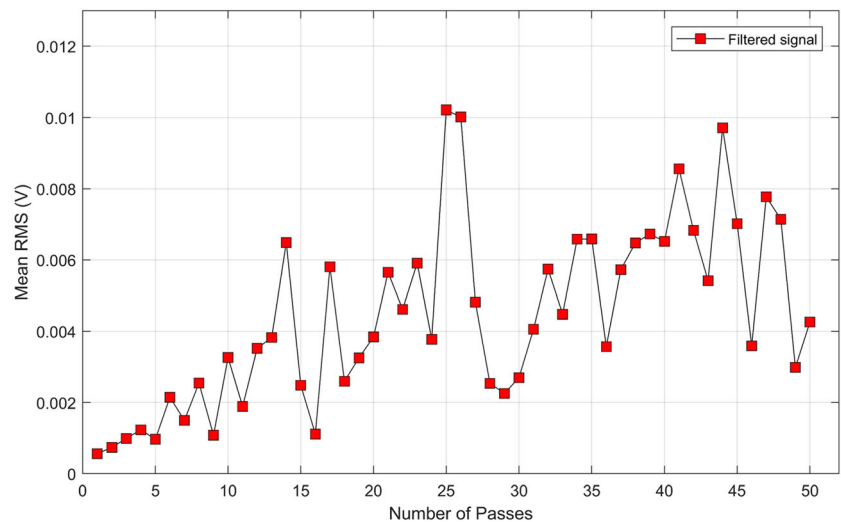
(a)
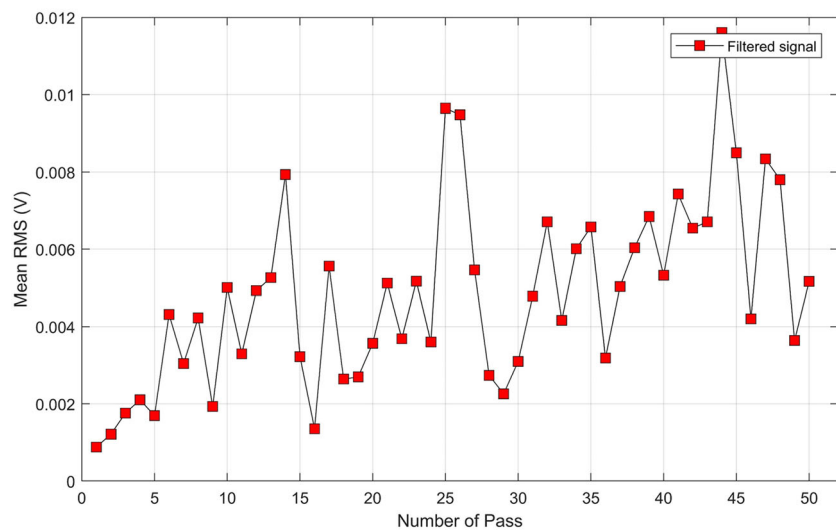
(b)

spacing between the peaks and the increase in the amplitude of the acoustic emission signal. This phenomenon occurs because the contact area between the surface of the grinding wheel and the multipoint diamond dresser is bigger. Lastly, it can be observed that by the end of the dressing process, on the 50th pass, the AE signal sampled does not have spacing between the peaks as observed in the previous passes. Besides that, the amplitude of the signal is bigger in comparison with the signal on the 4th and 28th passes. Again, the observed alterations occur in function of the contact area between the grinding wheel surface and the dresser. However, analyzing only the signal in the time domain is not possible to determine the optimum moment to interrupt the dressing process once the variations are gradual. In this way, it is necessary to apply statistics that can support on the diagnosis of the process and consequently, the condition of the wheel surface.

The statistics used to evaluate the acoustic emission signal of the dressing process are shown in Fig. 6. The RMS presents intervals with values close to zero due to the irregular contact area between the grinding wheel and the dresser. Moreover, through the RMS signal, it is possible to detect the beginning and end of the dressing pass, once it is identified an accentuated increase at 0.3 s and decrease at 3.3 s, when the dresser is not in contact with the grinding wheel anymore. The threshold used to contabilize counts in the sampled signals is also shown. The threshold was established 10% above the noise identified in the signal.

The RMS original signal averages are shown in Fig. 7. It observed an increase in the values as the dressing passes progress. However, the behavior observed does not show a linear trend, hindering the automatic diagnosis. The 25th and 26th passes present higher RMS average. However, the passes

number 27 to 31 show a decrease of the RMS average. This variation makes the system unfeasible for practical applications.

The counts averages for each dressing pass are presented in Fig. 8. In comparison with RMS (Fig. 7), it is possible to observe better performance of the counts statistics once there is a trend of increasing of the signal. However, the task of establishing a threshold that indicate the correct moment to interrupt the dressing process is hard due to the fact that the measurements does not show similar values. For instance, passes from number 43 to 47 present very close values, which might indicate that the wheel surface is in the desired condition. Passes from number 48 to 50 present random behavior, invalidating the surface diagnosis presented by the passes from 43 to 47. In this context, it is necessary that the study of the signal in the frequency domain aim to find frequency bands that are related to the process conditions. From the band

selection, digital filters can be used and the statistics reapplied on the filtered signal.

The frequency spectrum for the three dressing process condition is presented in Fig. 9a. It can be seen that most of the spectrum on pass number 50 has highest amplitude while the 4th pass has the lowest one. In this way, the more dressing passes are applied on the grinding wheel, the bigger will be the spectrum level. According to the criteria presented on the "Experimental setup" section, both frequency bands selected were 52–62 kHz and 110–118 kHz. A detailed analysis is presented on Fig. 9 b and c, respectively. It observed well marked behaviors for each condition of the process (beginning, middle, and end).

Figure 10 presents the average of the RMS filtered signal in each dressing pass. Figure 10a shows the average of the RMS signal filtered on 52 to 60 kHz band, while Fig. 10b presents

Fig. 11 Counts average of the filtered signal. **a** 52–60 kHz band. **b** 110–116 kHz band

(a)

(b)
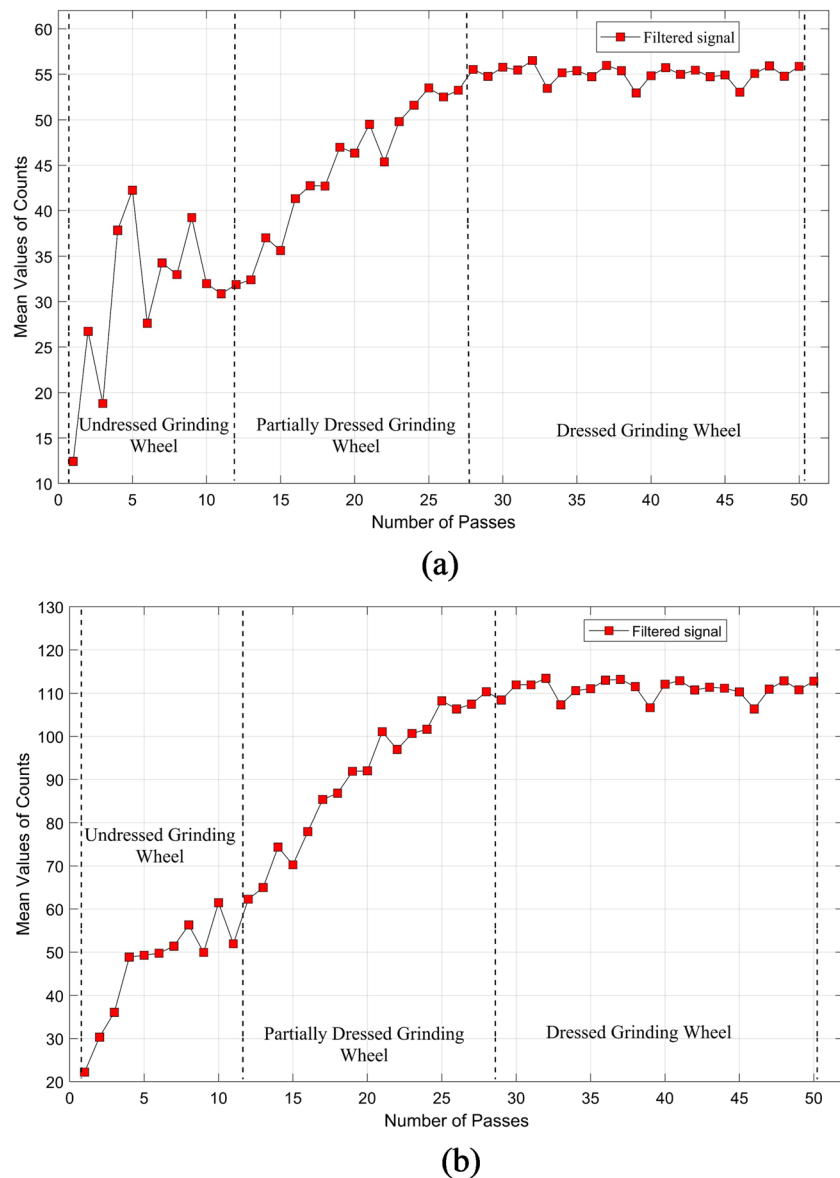
the average RMS filtered signal on 110 to 116 kHz band. Similarly to the results presented on Fig. 7, the RMS average of the filtered signal in both frequency bands present highly non-linear behavior, hindering the identification of patterns related to the process conditions. The similarity between the results can be explained due to use of multi-point dresser, which is a source of acoustic emission signal when the dresser is in contact with the grinding wheel. In this way, although the filter is applied on the entire AE sample signal, the energy level of the signal presents a similar behavior in all the frequency bands. In this way, it can be concluded that the RMS statistic have not presented sensibility to the diagnosis of the dressing process of CBN grinding wheels, implying in unfeasibility of the use of this system for automation of the dressing process.

The counts average of the filtered signal in both selected frequency bands for each dressing pass is shown in Fig. 11. Figure 11a presents counts average of the filtered signal in the 52–62 kHz band. Opposed to the results presented by the RMS average (Figs. 7 and 10) and by the *counts* average of the original signal (Fig. 8), it is possible to identify three regions as well-defined. The first region identified comprises passes 1 to 12 and represents the beginning of the dressing process, when the grinding wheel is clogged. The main characteristic of this region is the non-linear behavior of the measurements.

The second region identified, passes 13 to 28, is related to the middle of the dressing process and intermediate level of clogging of the grinding wheel, that is, there was removal of material of the grinding wheel surface during the dressing process, but it is not yet fit to be used again in the process since it is not in its best condition. The main characteristic of this region is the accentuated increase of the counts' statistic level. Lastly, the third identified region, passes 29 to 50, regard the end of the dressing process when the grinding wheel is fit to be used again. In this region, the main characteristic is

the similarity of the counts values. It should be noted that the counts average for the filtered signal on the 110–116 kHz band (Fig. 11b) present the same regions identified on Fig. 11a with the same characteristics previously described. The main difference identified consists of the counts statistic. It can be seen on Fig. 11a that the highest average presents value of 55 while on Fig. 11b the highest counts average has value of 115.

Lastly, from the results obtained of the counts average of the filtered signal in the selected bands of the dressing process, it is possible to see that it could be stopped about the 29th pass, saving time that was wasted with no gain in the process, as well as useful material that was removed from the surface of the grinding wheel, resulting in a lower total life of the tool. Besides that, the frequency bands analysis proves its importance when comparing the results presented in Fig. 11 with the results presented in Fig. 8 once the use of frequency bands allowed the identification of the conditions of the process. Thus, it should be noted that the boundaries of the regions presented in Fig. 11 a and b were made according to the characteristics of the values obtained with the counts statistics, in which the first region (unaddressed grinding wheel) presents variations and little stability. The second region (partially dressed grinding wheel) shows almost constant growth. Finally, the third region (dressed grinding wheel) presents stability in the counts values; that is, the values are very close when compared.

4.2 Results obtained with the analysis of the CBN GS (more friable) grinding wheel

4.2.1 Evaluation of the grinding wheel surface

The amplification of the surface of the GS wheel with clogging is presented in Fig. 12. Similarly to the results presented in Fig. 3 (GL wheel), it is not possible to identify the abrasive grains or pores of the wheel structure,
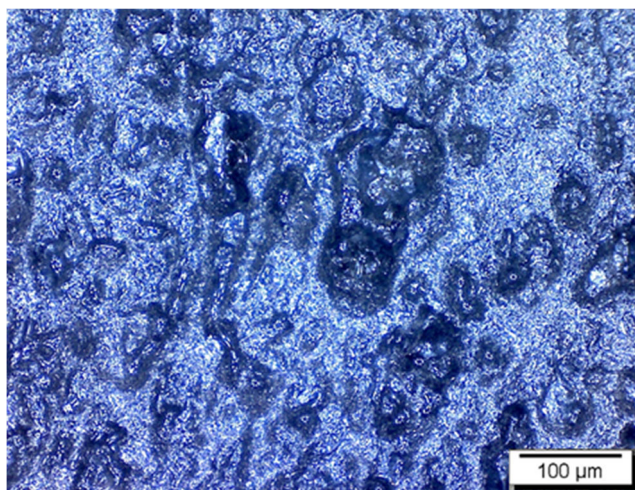

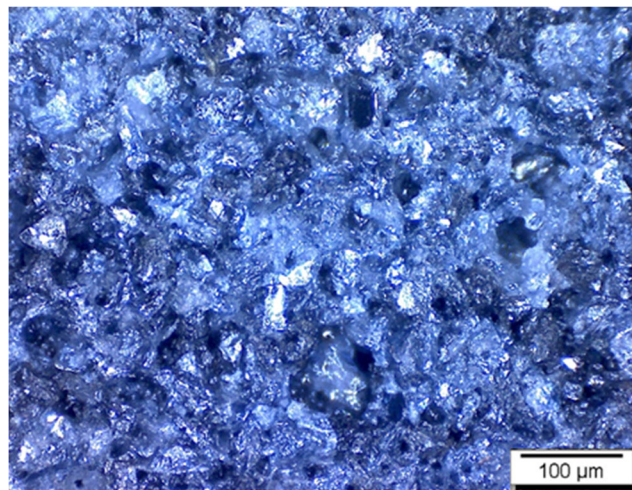**Fig. 12** Amplification of the clogged GS grinding wheel

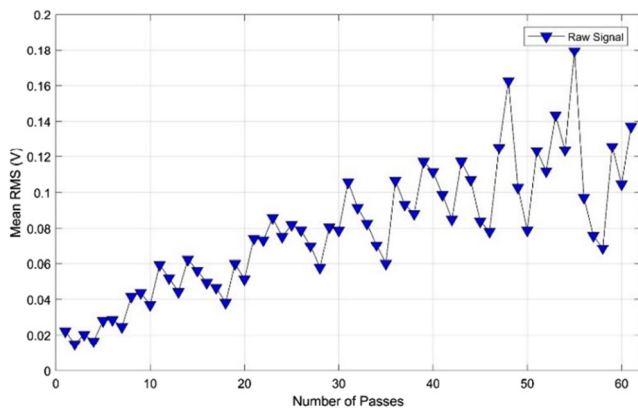**Fig. 13** Amplification of the dressed wheel

Fig. 14 RMS of the original signal

implying in a clogged surface, which makes the tool unfit to be used on the grinding process.

The surface of the GS grinding wheel after the dressing process is presented on Fig. 13, in which the abrasive grains can be seen. This image was obtained from the wheel surface after 61 dressing passes. The same observations as in Figs. 3 and 4 can also be applied, as they address the need to carry out a more significant amount of dressing to obtain a suitable topographic surface of the grinding wheel, resulting in the waste of abrasive material. In comparison with the GL wheel, there is a difference in the visual aspect since the more friable (GS) abrasive grains present a darker color while the less friable (GL) grains present amber color, which has higher contrast with the wheel structure, resulting in an easier identification of the grains.

The average of the RMS signal for each dressing pass is presented on Fig. 14. The trend of increase of the values as the dresser is moved in direction of the grinding wheel can be clearly seen. However, similarly to the analysis of the signal obtained with the GL grinding wheel, it is not possible to clearly and reliably identify the moments of the dressing

process and use it to determine the moment that the dressing of the wheel should be interrupted, for example. In this way, the RMS average of the AE signal is not a parameter fit to analyze the dressing process (at least for the CBN grinding wheel with multi-point dresser condition).

The counts average of the AE signal for each dressing pass is shown in Fig. 15. It can be observed a continuous trend of increase of the values with some little variations as the dresser is brought more in contact with the tool. Although the behavior presents a trend of values more reliable than the analysis presented in Fig. 14, it is not possible yet to identify the moment when the dressing process should be interrupted, when there should be no increase of value as the dresser is moved in direction of the grinding wheel, resulting in a different pattern in comparison with what was observed in Fig. 12 and the studies of some authors [32]. In this context, it is important to analyze the signal in the frequency scope, selecting the frequency bands that may characterize the process more efficiently.

The frequency spectrum of the AE signal for the three conditions of the dressing process is shown in Fig. 16. The analysis of the selected frequency bands is shown in Fig. 16 a and b. It can be seen that the process signal has different amplitudes in most of the spectrum. Besides that, the characteristics presented in Fig. 9a for the dressing process of GL wheel are also observed with the GS wheel, that is, the spectrum related to the beginning of the process has smaller amplitude (clogged wheel), while at the end of the process the amplitudes are bigger (dressed wheel). Two frequency bands were selected as follows: 66–70 kHz and 112–116 kHz.

Figure 17 presents the RMS average of the AE filtered signals on the selected bands, in which 66–70 kHz band is shown in Fig. 17a and 112–116 kHz band is shown in Fig. 17b. Similarly to the results obtained with the GL wheel, the RMS average of the dressing passes of the GS wheel does

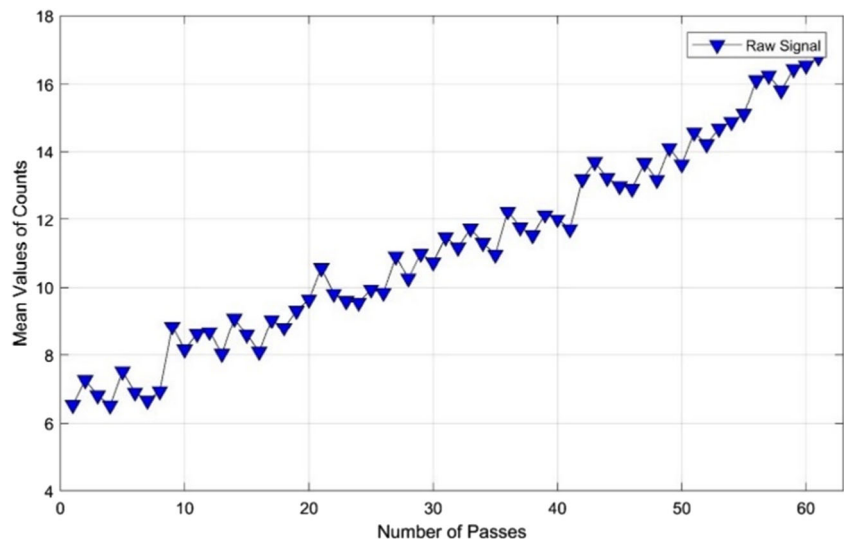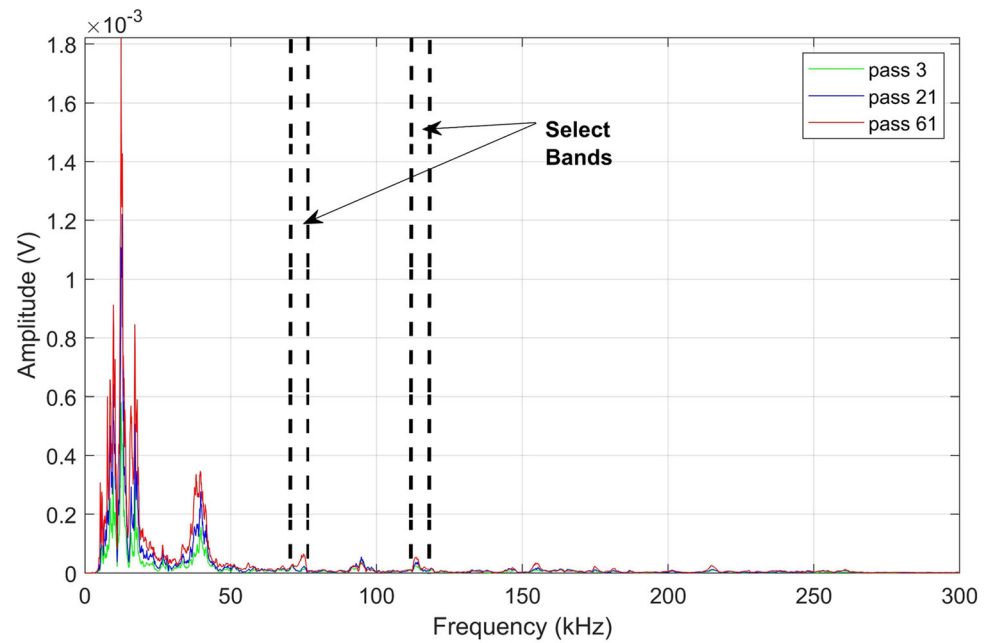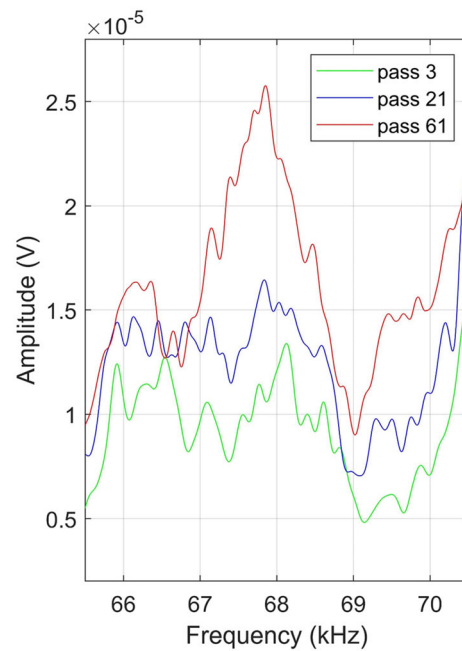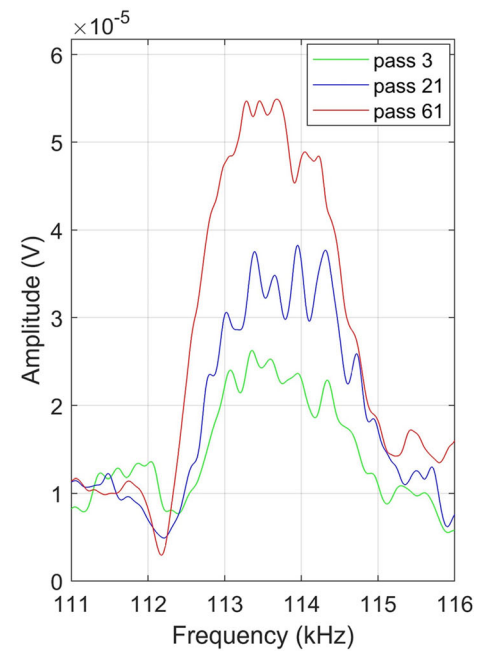**Fig. 15** Counts of the original signal

Fig. 16 Frequency bands selection


(a)

(b)

(c)

not present more homogeneous pattern. It can be seen some variations in comparison with the results obtained in Fig. 14, such as the difference on the amplitude of the average RMS values. However, it is not possible to define the optimum moment to interrupt the dressing process. In this way, the RMS average of the AE signal sampled during the process was not sensible to the variations of the process and surface condition of the wheel. This phenomenon imply in the

inability of the use of the RMS technique proposed in this work for applications to diagnose the dressing process of CBN wheel with multi-point dresser.

The counts average for the filtered signals on the frequency bands of 66–70 kHz and 112–115 kHz are presented in Fig. 18 a and b, respectively. In the same way of the results presented in Fig. 11 to GL grinding wheel, Fig. 19a presents three well-defined regions in which it is possible to diagnosis the wheel

Fig. 17 RMS filtered on the bands. **a** 66–70 kHz. **b** 112–115 kHz


(a)

(b)
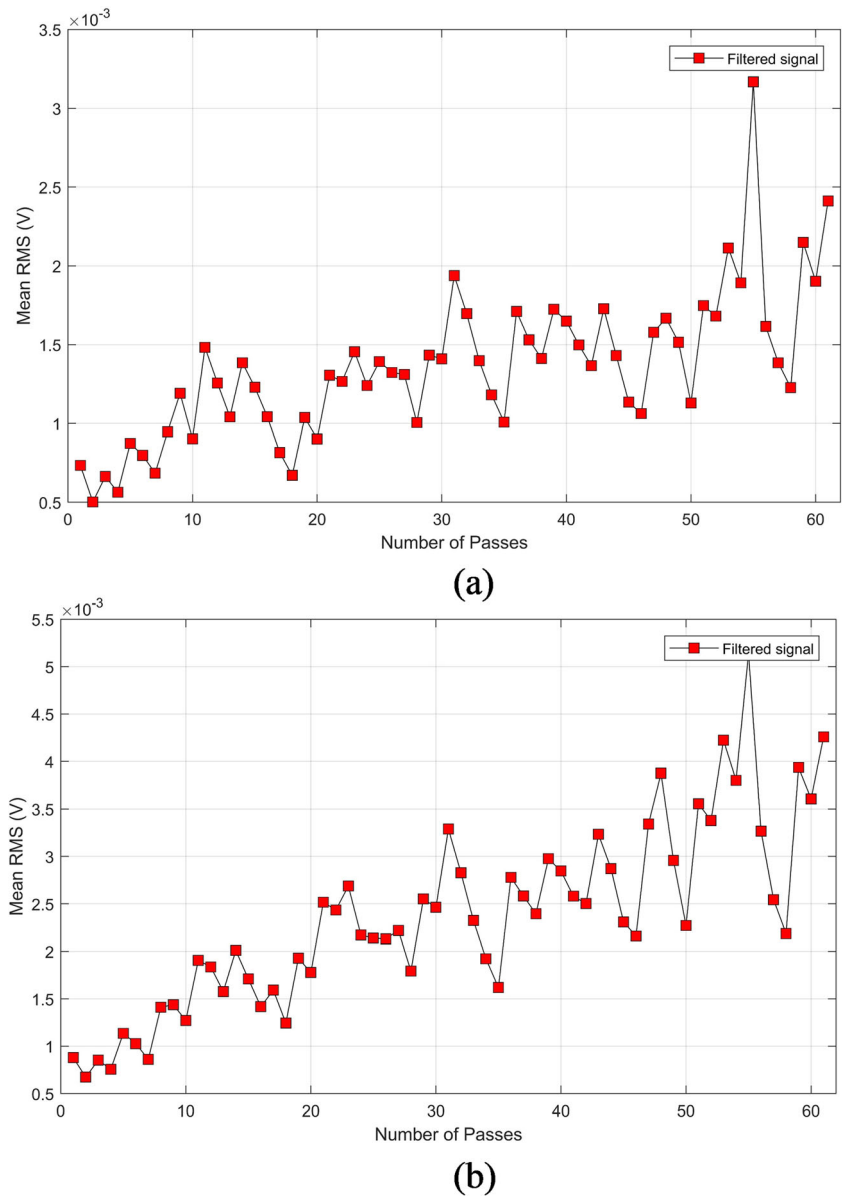
conditions during the process, in which the first refers to the clogged wheel in the beginning of the dressing process (passes from 01 to 09), intermediary condition (passes from 11 to 14) and finally clean surface, fit to be used on the grinding process (passes 45 to 61). The characteristics of the regions were similar to the observed in the GL wheel results, that is, initially there is no linearity of the values (grinding wheel before dressing), after that there is an accentuated increase of the signal (partially dressed) and finally there is stability of the values (dressed wheel). In this way, it is possible to establish the best moment to stop the dressing of the wheel in pass 45. Regarding Fig. 19b, the counts average of the filtered signal on the band 112 to 115 kHz presents the same regions. However, the selected pass for stopping the dressing process would be 51. Although different, both frequency bands could

be used on the diagnosis system. Due to the fact that the band 66 to 70 kHz presents the best performance, it could be used as main system, while the other band could be used for verification.

It should be highlighted that the differences found on the application of the technique in both grinding wheels can be explained in function of the different structures of the wheels. It could be noticed that the GL wheel (lower friability) is more fitted to be analyzed during dressing process with the proposed technique. Since its abrasive grains are less likely to be dislodged during dressing, the acoustic emission sources originated from the contact of the abrasive grains with the multi-point dresser are higher, favoring the application of counts statistics.

Fig. 18 Counts filtered on the band 112–115 kHz
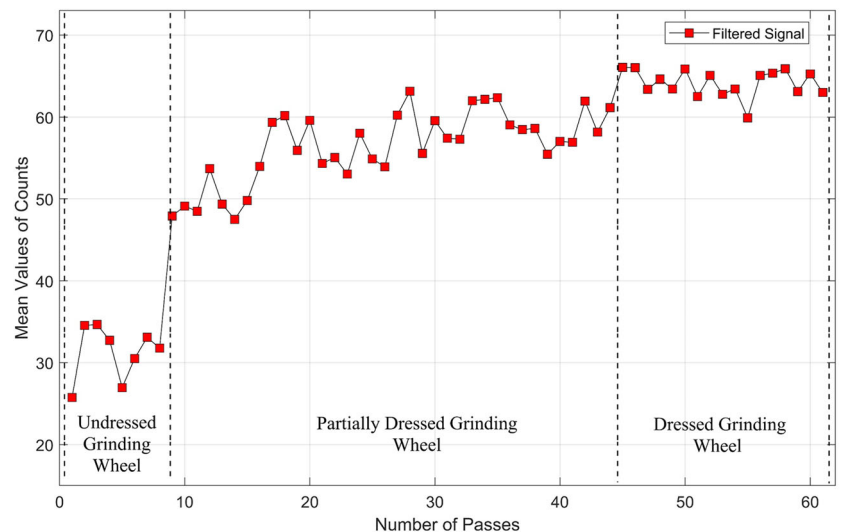
(a)
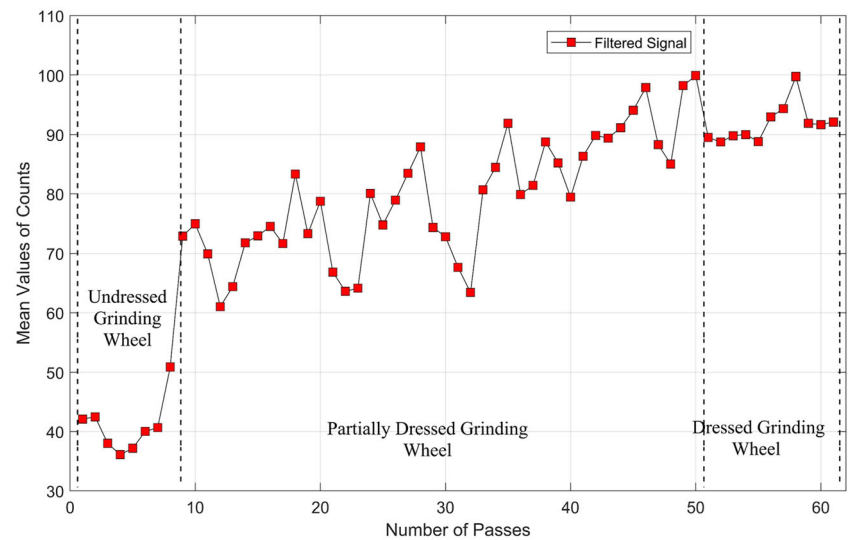
(b)

5 Conclusion

In this work, a technique to select the correct moment to stop the dressing process on CBN grinding wheels was proposed. An acoustic emission sensor, commonly used in process monitoring, along with techniques of digital processing of the signal were capable of identifying the characteristics of the process.

The results show that the average values of the RMS and counts statistics of the original signal were not capable of identifying the characteristics of the dressing process that should show a trend in intensity according to the surface condition, making unfeasible its acquisition and analysis for this purpose. However, after selecting the frequency band that is strongly related to the characteristics of the dressing process and applying digital filters on the original signal, the average

values of the counts statistics showed to be efficient to diagnosis the best moment to stop the dressing process. It is important to highlight that the RMS statistics was not sensitive to detect the characteristics of the dressing process, even after the original signal was filtered on the selected frequency bands.

The verification of the method in two CBN grinding wheels with similar structure but different abrasive grains and friability showed distinct results. However, the technique showed to be effective on both conditions and through the counts statistics, it was possible to determinate the best moment to stop the dressing process. In this way, the proposed technique can be applied on the dressing process of CBN. The generalization of this methodology can be applied through the selection of proper frequency bands that are strongly related with the characteristics of the process.

Finally, the authors suggest as future work the use of tools that allow a sufficient verification of the surface condition of the grinding wheels, helping in a more accurate correlation with the variations of the acoustic emission signals obtained during the dressing process monitoring. One can cite as an example of the use of laser micrometers.

Compliance with ethical standards

Conflict of interest The authors declare that they have no conflict of interest.

References

1. Li Z, Wang Y, Wang K-S (2017) Intelligent predictive maintenance for fault diagnosis and prognosis in machine centers: industry 4.0 scenario. Adv Manuf 5(4):377–387

2. Rodriguez RL et al (2019) Evaluation of grinding process using simultaneously MQL technique and cleaning jet on grinding wheel surface. J Mater Process Technol 271(October 2018):357–367

3. Wang Y, Ma H-S, Yang J-H, Wang K-S (2017) Industry 4.0: a way from mass customization to mass personalization production. Adv Manuf 5(4):311–320

4. Bianchi EC et al (2018) Evaluating the effect of the compressed air wheel cleaning in grinding the AISI 4340 steel with CBN and MQL with water. Int J Adv Manuf Technol 95(5–8):2855–2864

5. Alexandre FA et al (2018) Tool condition monitoring of aluminum oxide grinding wheel using AE and fuzzy model. Int J Adv Manuf Technol 1:1–13

6. Jiang JLL, Ge PQQ, Bi WBB, Zhang L, Wang DXX, Zhang Y (2013) 2D/3D ground surface topography modeling considering dressing and wear effects in grinding process. Int J Mach Tools Manuf 74:29–40

7. Alexandre FA, Lopes WN, Ferreira FI, Dotto FRL, de Aguiar PR, Bianchi EC (2017) Chatter vibration monitoring in the surface grinding process through digital signal processing of acceleration signal. Proceedings, 2(3):126

8. Aulestia Viera MA, Alexandre FA, Aguiar PR, Silva RB, Bianchi EC (2018) Correlation between surface roughness and AE signals in ceramic grinding based on spectral analysis. In: MATEC Web of Conferences, vol 249

9. Talon AG et al (2019) Effect of hardened steel grinding using aluminum oxide wheel under application of cutting fluid with corrosion inhibitors. Int J Adv Manuf Technol 104(1–4):1437–1448

10. de Mello HJ et al (2018) Contribution to cylindrical grinding of interrupted surfaces of hardened steel with medium grit wheel. Int J Adv Manuf Technol 95(9–12):4049–4057

11. Bianchi EC et al (2019) Application of the auxiliary wheel cleaning jet in the plunge cylindrical grinding with minimum quantity lubrication technique under various flow rates. Proc Inst Mech Eng B J Eng Manuf 233(4):1144–1156

12. Alexandre F et al (2018) Damage detection in grinding of steel workpieces through ultrasonic waves. MATEC Web Conf 249:02002

13. Javaroni RL et al (2019) Minimum quantity of lubrication (MQL) as an eco-friendly alternative to the cutting fluids in advanced ceramics grinding. Int J Adv Manuf Technol

14. Bianchi EC et al (2018) Plunge cylindrical grinding with the minimum quantity lubrication coolant technique assisted with wheel cleaning system. Int J Adv Manuf Technol 95(5–8):2907–2916

15. Winter M, Li W, Kara S, Herrmann C (2014) Determining optimal process parameters to increase the eco-efficiency of grinding processes. J Clean Prod 66:644–654

16. Dotto FRL et al (2019) Acoustic image-based damage identification of oxide aluminum grinding wheel during the dressing operation. Procedia CIRP 79:298–302

17. Junior P, D'Addona D, Aguiar P, Teti R (2018) Dressing tool condition monitoring through impedance-based sensors: part 2—neural networks and k-nearest neighbor classifier approach. Sensors 18(12):4453

18. Junior PO et al (2019) Impedance-based PZT transducer and fuzzy logic to detect damage in multi-point dressers. In: Gapiński B, Szostak M, Ivanov V (eds) Advances in manufacturing II, 4th edn. Springer, Cham, pp 213–222

19. de Martini Fernandes L et al (2019) Thermal model for surface grinding application. Int J Adv Manuf Technol

20. Lopes JC et al (2018) Application of minimum quantity lubrication with addition of water in the grinding of alumina. Int J Adv Manuf Technol 97(5–8):1951–1959

21. Lopes JC et al (2019) Application of a wheel cleaning system during grinding of alumina with minimum quantity lubrication. Int J Adv Manuf Technol 102(1–4):333–341

22. Rodriguez RL et al (2019) Contribution for minimization the usage of cutting fluids in CFRP grinding. Int J Adv Manuf Technol 103(1–4):487–497

23. Kalpakjian S, Schmid SR (2014) Manufacturing engineering and technology, 7th edn. Pearson Education South Asia Pte Ltd, Singapore

24. Palmer J, Ghadbeigi H, Novovic D, Curtis D (2018) An experimental study of the effects of dressing parameters on the topography of grinding wheels during roller dressing. J Manuf Process 31:348–355

25. Badger J, Murphy S, O'Donnell GE (2018) Acoustic emission in dressing of grinding wheels: AE intensity, dressing energy, and quantification of dressing sharpness and increase in diamond wear-flat size. Int J Mach Tools Manuf 125:11–19

26. Holesovsky F, Pan B, Morgan MN, Czan A (2018) Evaluation of diamond dressing effect on workpiece surface roughness by way of analysis of variance. Teh Vjesn Tech Gaz 25(Supplement 1):165–169

27. Lopes JC et al (2019) Effect of CBN grain friability in hardened steel plunge grinding. Int J Adv Manuf Technol 103(1–4):1567–1577

28. Marinescu I, Hitchiner M, Uhlmann E, Rowe WB, Inasaki I (2006) Handbook of machining with grinding wheels, Boca Raton

29. Martins CHR, Aguiar PR, Frech A, Bianchi EC (2014) Tool condition monitoring of single-point dresser using acoustic emission and neural networks models. IEEE Trans Instrum Meas 63(3):667–679

30. da Conceição Junior PO, Ferreira FI, de Aguiar PR, Batista FG, Bianchi EC, DAddona DM (2018) Time-domain analysis based on the electromechanical impedance method for monitoring of the dressing operation. Procedia CIRP 67:319–324

31. Conceição Junior PDO et al (2018) A new approach for dressing operation monitoring using voltage signals via impedance-based structural health monitoring. KnE Eng 3(1):942

32. Nascimento Lopes W et al (2017) Digital signal processing of acoustic emission signals using power spectral density and counts

statistic applied to single-point dressing operation. IET Sci Meas Technol 11(5):631–636

33. Junior P, D'Addona DM, Aguiar PR (2018) Dressing tool condition monitoring through impedance-based sensors: part 1—pzt diaphragm transducer response and emi sensing technique. Sensors 18(12):4455

34. Lauro CH, Brandão LC, Baldo D, Reis RA, Davim JP (2014) Monitoring and processing signal applied in machining processes - a review. Meas J Int Meas Confed 58:73–86

35. Alexandre FA, Aguiar PR, Götz R, Aulestia Viera MA, Lopes TG, Bianchi EC (2019) A novel ultrasound technique based on piezoelectric diaphragms applied to material removal monitoring in the grinding process. Sensors 19(18):3932

36. Teti R, Jemielniak K, O'Donnell G, Dornfeld D (2010) Advanced monitoring of machining operations. CIRP Ann Manuf Technol 59(2):717–739

37. Webster J, Dong WP, Lindsay R (1996) Raw acoustic emission signal analysis of grinding process. CIRP Ann Manuf Technol 45(1):335–340

38. Lopes WN et al (2018) Monitoring of self-excited vibration in grinding process using time-frequency analysis of acceleration signals. In: 2018 13th IEEE International Conference on Industry Applications (INDUSCON), pp 659–663

39. Lopes BG, Alexandre FA, Lopes WN, de Aguiar PR, Bianchi EC, Viera MAA (2018) Study on the effect of the temperature in Acoustic Emission Sensor by the Pencil Lead Break Test. In: 2018 13th IEEE International Conference on Industry Applications (INDUSCON), pp 1226–1229

40. Alexandre F et al (2018) Emitter-receiver piezoelectric transducers applied in monitoring material removal of workpiece during grinding process. Proceedings 4(1):9

41. Junior POC et al (2019) Feature extraction using frequency spectrum and time domain analysis of vibration signals to monitoring advanced ceramic in grinding process. IET Sci Meas Technol 13(1):1–8

42. Viera MAA et al (2019) Low-cost piezoelectric transducer for ceramic grinding monitoring. IEEE Sensors J 19(17):7605–7612

43. Viera M et al (2018) A contribution to the monitoring of ceramic surface quality using a low-cost piezoelectric transducer in the grinding operation. In: Proceedings of 5th International Electronic Conference on Sensors and Applications, p 5733

44. Thomazella R, Lopes WN, Aguiar PR, Alexandre FA, Fiocchi AA, Bianchi EC (2019) Digital signal processing for self-vibration monitoring in grinding: a new approach based on the time-frequency analysis of vibration signals. Measurement 145:71–83

45. Aulestia Viera MA et al (2019) A time–frequency acoustic emission-based technique to assess workpiece surface quality in ceramic grinding with pzt transducer. Sensors 19(18):3913

46. Ribeiro DMS, Aguiar PR, Fabiano LFG, D'Addona DM, Baptista FG, Bianchi EC (2017) Spectra measurements using piezoelectric diaphragms to detect burn in grinding process. IEEE Trans Instrum Meas 66(11):3052–3063

47. Euzebio CDG et al (2012) Monitoring of grinding burn by fuzzy logic. ABCM Symp Ser Mechatron 5:637–645

48. M. Kaphle, "Analysis of acoustic emission data for accurate damage assessment for structural health monitoring," 2012

49. Wegener K, Hoffmeister HW, Karpuschewski B, Kuster F, Hahmann WC, Rabiey M (2011) Conditioning and monitoring of grinding wheels. CIRP Ann Manuf Technol 60(2):757–777

50. Inasaki I, Okamura K (1985) Monitoring of dressing and grinding processes with acoustic emission signals. CIRP Ann 34(1):277–280

51. Inasaki I (1999) Sensor fusion for monitoring and controlling grinding processes. Int J Adv Manuf Technol 15(10):730–736

52. Karpuschewski B, Wehmeier M, Inasaki I (2000) Grinding monitoring system based on power and acoustic emission sensors. CIRP Ann Manuf Technol 49(1):235–240

53. Caggiano A, Teti R (2013) CBN grinding performance improvement in aircraft engine components manufacture. Procedia CIRP 9:109–114

54. Chiu N-H, Guao Y-Y (2008) State classification of CBN grinding with support vector machine. J Mater Process Technol 201(1–3):601–605

55. de Martini Fernandes L et al (2018) Comparative analysis of two CBN grinding wheels performance in nodular cast iron plunge grinding. Int J Adv Manuf Technol 98(1–4):237–249

56. Alexandre F et al (2018) Emitter-receiver piezoelectric transducers applied to material removal monitoring in grinding process. In: Proceedings of 5th International Electronic Conference on Sensors and Applications, p 5732

57. Ribeiro DMS, Conceição PO Jr, Sodário RD, Marchi M, Aguiar PR, Bianchi EC (2015) Low-cost piezoelectric transducer applied to workpiece surface monitoring in grinding process. ABCM Int Congr Mech Eng COBEM 23(1–10)